

ADDUCT: Aerobrake Deorbit Device for a 1U Cubesat

James Kilroe¹, Peter Martinez¹

¹*SpaceLab, University of Cape Town, South Africa*

jameskilroe@gmail.com

Keyword: Orbital Debris, 1U Cubesat, Aerobrake Deorbit Device, On-Orbit Deployment

Introduction

During the first decades of the Space Age, satellite development activities witnessed a remarkable growth in the size, complexity and capability of satellites. Modern multipurpose satellites can weigh several tons and cost hundreds of millions of dollars. However, as technology has improved, it has also become possible to develop much smaller satellites with capabilities previously only available on the larger satellites. Small satellites have a number of operational advantages compared to large satellites; these include the possibility of constellations for Earth observation or communication. Due to their reduced cost, nano-satellites can be used for on-orbit technology demonstrations. These small satellites are often launched as secondary payloads that take up unused capacity in a launcher being used to deliver a large satellite to orbit. This, in turn, has reduced the cost required to launch such small satellites. These small satellites are typically less than 500 kilogrammes in mass and fall into a number of sub-categories ranging from micro-satellites to nano-satellites, which are less than 10 kilogrammes.

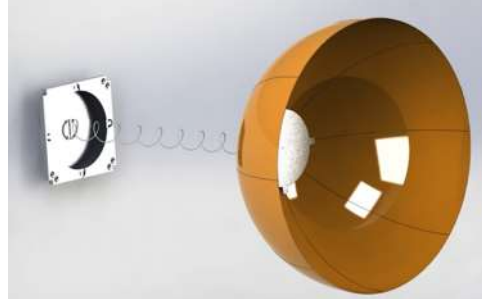
Orbital crowding is a problem that will become more serious as more Cubesats are launched into orbits with decay times greatly exceeding their predicted operational lifetimes. If a critical threshold of launches is exceeded, there is a significant risk of the Kessler Syndrome occurring, which is when collisions among space objects generate debris faster than it can be removed through natural orbital decay processes (Kessler and Cour-Palais, 1978). The aim of this paper is to describe the design of a device which aims to decrease the orbit decay time of a 1U Cubesat to within the 25-years recommended by the Inter-Agency Debris Coordination Committee (IADC) (IASDCC, 2014).

1U Cubesats were chosen as the topic of this project due to their growing popularity among emerging space actors. As of 20 May 2015, 125 1U Cubesats have been launched compared to the total number of 324 Cubesats, which is 39% (Swartwout, 2014). This paper describes the development of the ADDUCT device to a Technology Readiness Level of 4. This includes the simulations and terrestrial testing that the device underwent to ensure that it will be able to deorbit the Cubesat within the required 25-year time frame. In order to make this device feasible for 1U Cubesats, the device aimed to occupy less than 0.1U of usable Cubesat volume.

Design of ADDUCT Device

The design concept of the ADDUCT device is shown in Figure 1. It features a parabolic sail, a Nitinol helical boom, and a stepped housing. The parabolic sail shape provides passive attitude stability, as the Nitinol helical boom separates the centre of pressure and centre of mass of the Cubesat, which increases the aerodynamic torque. Thus, the sail shape is inclined to maximise the projected area relative to the velocity. The sail will be rigidised using thin nitinol wire; this will allow it to regain its parabolic shape using the unique shape memory properties of Nitinol. The disadvantage of this sail shape is the extra sail material required that would not increase the frontal surface area directly. Secondly, this shape is more difficult to obtain through deployment, and thus Nitinol wire is required to rigidise the sail. This increases the complexity of the device.

Figure 1: Design concept of the ADDUCT device



Fundamental physics of orbital decay

This deorbiting method uses the residual atmosphere to deorbit the Cubesat; as such, the projected area critically affects the effectiveness of the device, due to the drag force equation (Douglas et al., 2011).

$$F_D = 1/2 \cdot \rho_{\text{Air}} \cdot V^2 \cdot A \cdot C_d \quad (1)$$

where: F_D = drag force, ρ_{Air} = air density, V = velocity of the satellite relative to fluid, A = projected area parallel to the direction of motion, C_d = drag coefficient. As can be seen from Equation 1, the projected area A of a satellite relative to its direction of flight is one of the contributors to the drag force. Therefore, any aerobraking mechanism should seek to maximise the projected area A in the direction of flight. This requires an ability to control the orientation of the satellite, either passively or actively. Ideally, the deorbiting mechanism will orientate the spacecraft in a passive manner. An advantage of the altitude control being performed by the deorbiting mechanism is that there will be no additional requirements on the Cubesat. This allows for potential integration of the ADDUCT device onto a number of different Cubesats. Another advantage of ensuring passive control is that there is no risk of a control system/electronic failure causing the satellite to tumble and the deorbit device to become ineffective. Furthermore, the device could be deployed at the beginning of the mission to assist with the orientation of the device throughout the mission.

Passive attitude stabilisation

Passive stabilisation is achieved using the environmental forces that are exerted on the satellite to orientate the satellite. The satellite will tend to orientate itself to minimise the torques exerted on it. These include four major induced torques from external forces: Gravity gradient forces, Aerodynamic forces, Magnetic forces, and Solar pressure.

The total torque is a combination of the individual torques:

$$T_{\text{total}} = T_{\text{gg}} + T_{\text{aero}} + T_{\text{coils}} + T_{\text{hysteresis}} \quad (2)$$

These torques affect the satellite differently at different heights. Furthermore, these forces can change periodically as the atmosphere and solar winds change in intensity. This makes calculating the exact total torque difficult. Table 1 characterises these environmental perturbations in terms of dominant regions of influence (Rawashdeh, 2012). Cubesats are most commonly found in Regions 1-2. To increase the aerodynamic torque, the centre of pressure (CP) and centre of mass (CM) need to be separated; for stable flight, the CM should be in front of the CP. For a Cubesat, the adjustment of CM and CP has to be done post-deployment because, due to the Cubesat standard, the CM has to be within a 2-cm radius of the centre of the Cubesat at launch. The moment of the aerodynamic torque is shown in Figure 2.

Figure 2 (Below left): Aerodynamic torque experienced by a Cubesat in orbit. The moment arm is the distance between the centre of mass and the centre of pressure. The aerodynamic torque will tend to orient the satellite in the direction of the velocity vector

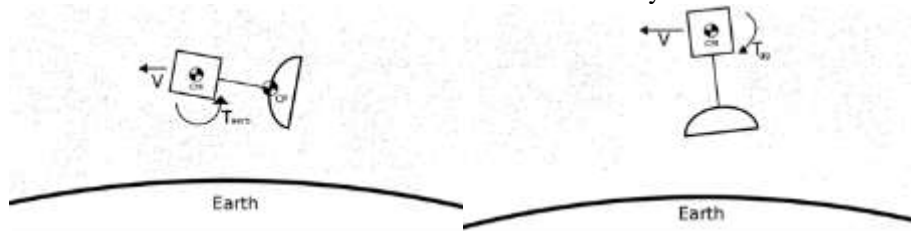


Figure 3 (Above right): The gravity gradient torque tends to align the long axis of a satellite along a line pointing towards Earth's centre of mass i.e. perpendicular to the orbital velocity vector

Table 1: Environmental Torques Regions of Influence. Adopted from Rawashdeh, (2012) and Montenbruck and Gill, (2000).

Region of Influence	Dominate Environmental Effects
Region 1 - Below 300 km	Aerodynamic torque
Region 2 - 300-850 km	Aerodynamic & Gravitational torques
Region 3 - 850-1000 km	Aerodynamic, Gravitational & Solar Torques
Region 4 - Above 1000km	Solar & Gravitational Torques

Calculations were performed to compare the aerodynamic and gravity gradient torques, whose default orientation is shown in Figure 3. Table 2 shows that the aerodynamic force overcomes the gravity gradient

force at altitudes lower than 700km. Thus, this device could be used to passively orientate the craft below 700km.

Table 2: Aerodynamic and gravity gradient torques at different orbital heights

Orbital Heights (km)	Aerodynamic Torque (N.m)	GG Torque (N.m)	Orbital Heights (km)	Aerodynamic Torque (N.m)	GG Torque (N.m)
900	4.56×10^{-10}	5.78×10^{-9}	800	2.51×10^{-9}	6.01×10^{-9}
700	1.39×10^{-8}	6.26×10^{-9}	600	7.64×10^{-8}	6.52×10^{-9}
500	4.22×10^{-7}	6.79×10^{-9}	400	2.33×10^{-6}	7.08×10^{-9}
300	1.28×10^{-5}	7.38×10^{-9}			

Deorbiting Properties

The effective sail area is the projected area of the sail relative to the velocity vector and not its total surface area. The orbital lifetime predictor tool from STK was used to investigate the effect of increasing a 1U Cubesats surface area on its orbital life (AGI, 2016). The following variables were set constant at: Atmospheric model = Jacchia 1970 Lifetime, Solar flux data = Latest Available, Satellite mass = 1.33 kg, Drag coefficient = 2.2, Reflection coefficient = 1.0, Cross-sectional area = 0.06 m². Area exposed to sun = Cross-sectional area. A 0.06m² sail is suitable because, as shown in Table 3, the device deorbits the Cubesat in 6 years. Due to its smaller size, its housing would have the least impact on the limited available volume for a 1U Cubesat.

Table 3: Results of STK Orbital Lifetime Tool prediction in years for a 1U Cubesat.

Launch date	21:00:00 UTC, October 21, 2018	Semi-Major Axis	6930 km
Orbital Inclination	97.6 degree	Eccentricity	0.02
R.A.A.N	30 degree	Argument of Perigee	210 degree
Mean Anomaly	190 degree	Predicted Lifetime	6.0 years

Design and construction of sail

As shown in Figure 1, the sail shape is a half hemispheric shape. The curved sail shape increases the radar cross-section and passive aerodynamic torque, and this is considered a major advantage of this shape. The diameter of the hemisphere is determined to be 28cm. This allows for the cross-sectional area to exceed 0.06m². In order to achieve the hemispherical shape, it was decided to create eight sail sections called gores. The eight gores of the sail are constrained by four Nitinol Φ0.5mm wire frames. The prototype sail material was selected to be Kapton 50HN. The sail construction was performed by hand and involved three steps. These were constructing the Nitinol frame, cutting the gores and constructing the sail. The eight gores were laser cut out of Kapton 50HN. The sail was manufactured using the gores and Nitinol sail frames. Once the Nitinol frames were manufactured, the gores were taped to the frames using Kapton tape. Figure 2 shows the completed sail.

Figure 2: The completed Kapton sail constructed out of eight gores.



Electrical design of the ADDUCT Device

The deployment of our sail requires heating of the Nitinol helical boom and sail frame. We investigated several possible approaches to heating the wires and chose a Pulse Width Modulation (PWM) approach as opposed to a Direct Current (DC) approach. There was a myriad of different reasons for this option, with the primary reason being the uniformed heating experienced under PWM. The electrical requirements for the device are shown in

Table 4 and include the small electrical requirements of the burn wire release mechanism.

Table 4: Electrical Requirements of ADDUCT Device

	Burn Wire	Helical Boom	Four sail frames
Voltage (V)	0.16	1.86	4.4
Average Current (A)	1	1.5	1.5
Total Energy (watt.hours)		0.310	

Design of the sail housing

During the conceptual design stage, a stepped horizontal tray shape was selected as the optimal shape for the sail housing. This was because the shape allows for the minimising of wasted space and the simplification of the modular integration of the ADDUCT system with the rest of the satellite. The basic layout of the sail housing is a central circular well of 80mm diameter and 13mm depth in which the sail is stowed. The deployment mechanism and associated electrical components occupy the peripheral space around the central well. The Cubesat standard dimensions determined the dimensions. This determined the outer dimensions of the housing, which is square with 98mm sides. The height of the ADDUCT device was 16.28mm, from the cover plate to the bottom of the sail housing. The square stepped section of the sail housing was 6.28mm and is designed to occupy the 7mm between the Cubesat body and top of Cubesat legs. Table 5 shows the mass budget of the ADDUCT device. The total mass of this version was 128.0 gram.

Figure 3 (Below left): A rendered top view of the sail housing showing the central sail stowage well, surrounded by a circular channel to accommodate the release mechanism.



Figure 4 (Above right): A view of the cover lid, secured in place on the sail housing by a Nylon cable, that runs over the four projecting tabs on the lid. A burn wire is routed in the circular channel in the sail housing. The burn wire is set to have four burn locations corresponding to the four points at which the Nylon cable holds down the lid.

Table 5: Mass budget of the ADDUCT Device

Component	Mass (g)	Component	Mass (g)
Housing	88.7	Sail Fastener	1.7
Sail	11.0	Nitinol Helical Boom	4.5
Lid	12.3	Cover plate	9.8
Total	128.0		

Design of the release mechanism

A spring-and-cable concept was selected as the final release mechanism, as it was tested and determined to work reliably. It used Nylon rope to secure the lid onto the sail housing at four points around its circumference. When a current was applied to a burn wire, the Nylon was melted at the four different locations and the cable was released. In order to reduce the risk of failure, the cable was a single piece of Nylon and it was determined experimentally that only two out of the four burn locations were required to work to release the lid successfully. Figure 4 shows the Nylon rope holding the lid down as well as the routing of the burn wire, which was routed through the outer circular groove situated in the body of the sail housing. This mechanism was tested many times, but only failed to release when the Nylon rope was intentionally severed in only one location.

Testing Results

An air table was used to simulate the micro-gravity conditions under which the ADDUCT device is designed to operate. The test setup was arranged to allow the horizontal deployment of the Nitinol helical boom and the unfurling of the sail to be deployed, without gravity influencing the result. A number of different subsystem tests were conducted in order to test the different deployment stages of the ADDUCT device. The final integration test involved demonstrating that the release mechanism worked. Following this, that the Nitinol helical boom deployed when electrical current was supplied to it and finally the sail was deployed.

Figure 5 was taken after the burn wire had severed the Nylon line. The normal force of the compressed sail partially ejected the Lid from the sail housing, without the Nitinol helical boom being deployed. Figure 6 shows the device once the Nitinol helical boom had been deployed; one can see that it is been offset from the sail housing by over 240mm. Figure 7 is an image of the fully deployed sail, which was deployed using PWM current.

Conclusion

The ADDUCT device can effectively provide passive stability and deorbit a 1U Cubesat from a nominal orbit within 6.0 years. Furthermore, the shape will increase the radar cross-section of the device, which will assist in tracking it. The final mass of the proof-of-concept ADDUCT device was 128.0 grams. It is expected that the flight version will have a reduced mass as the sail housing will be milled out. The stowed device can fit within the Cubesat envelope prior to launch. The first flight edition will be connected to the Cubesat power system and deployed by the Cubesat power board; this means the device will be completely passive at launch. It is envisaged that a future educational flight version will be able to completely self-deploy with its only requirements being that it must be mounted before launch and that a ‘remove before flight’ pin must be pulled. For this version, the electrical subsystem would have to be installed in the housing of the ADDUCT device. This will reduce its dependency on untested educational Cubesats and thus provide a reliable deorbit method. The total cost of the prototype device was \$482, with the project cost so far being \$895. The energy budget to deploy the device is roughly 1% of a typical Cubesat’s battery capacity. Furthermore, the maximum peak current required is 3A less than the maximum current available in Cubesats, which is 4A. Lastly, the ADDUCT device will not generate any additional debris as all parts of the device remained secured to the Cubesat.

Figure 5 (Below left): The compressed sail ejecting itself once the burn wire was activated.



Figure 6 (Above middle): The deployment of the Nitinol helical boom by over 240 mm.

Figure 7 (Above right): The unfurled sail, which was deployed using PWM.

References

- AGI (2016) *Systems Tool Kit*. Available at: <http://www.agi.com/products/stk/>.
- Douglas, D. J. F. et al. (2011) *Fluid Mechanics*. 6 edition. Harlow, England ; New York: Prentice Hall.
- IASDCC (2014) *Support to the IADC Space Debris Mitigation Guidelines*. Available at: <http://www.iadc-online.org/Documents/IADC-04-06%20Support%20to%20IADC%20Guidelines%20rev5.5.pdf>.
- Kessler, D. J. & Cour-Palais, B. G. (1978) 'Collision frequency of artificial satellites: The creation of a debris belt'. *Journal of Geophysical Research*, 83(A6), pp. 2637. doi:10.1029/JA083iA06p02637.
- Montenbruck, O. & Gill, E. (2000) *Satellite Orbits*. Berlin, Heidelberg: Springer Berlin Heidelberg. Available at: <http://link.springer.com/10.1007/978-3-642-58351-3> (Accessed: 25 March 2016).
- Rawashdeh, S. (2012) *CubeSat Aerodynamic Stability at ISS Altitude and Inclination*. Available at: <http://digitalcommons.usu.edu/smallsat/2012/all2012/68/> (Accessed: 24 March 2016).

Swartwout, M. (2014) *The First 272 CubeSats*. Google Docs, Available at:
https://drive.google.com/file/d/0B_YNiLtqhzSqOGtYQTc5NHpmdzg/edit?pli=1 (Accessed: 24 March 2016).